

Removal of Bismarck Brown and Disulfine Blue from Aqueous Solutions Using MWCNTs Functionalized by N-(3-nitrobenzylidene)-N'-trimethoxysilylpropyl-ethane-1,2-diamine

Alireza Geramizadegan*

Department of Chemistry, Dashtestan Branch, Islamic Azad University, Dashtestan, Iran

Received April 2023; Accepted May 2023

ABSTRACT

The applicability of N-(3-nitro-benzylidene)-N'-trimethoxysilylpropyl-ethane-1,2-diamine onto multi walled carbon nanotubes (NBATSPED-MWCNTs) for removing Bismarck Brown and Disulfine Blue from aqueous solutions has been reported. This novel material was characterized by different techniques such as XRD, SEM and FT-IR. The influence of nanoparticle dosage, pH of the sample solution, individual dyes concentration, contact time between the sample and the adsorbent, temperature, and ionic strength of the sample solution were studied by performing a batch adsorption technique. The maximum removal of 15 mg L⁻¹ of individual dyes from an aqueous sample solution at pH 8.0 for Bismarck Brown (BB) and at pH 6.0 for Disulfine Blue (DSB) was achieved within 65 min when an adsorbent amount of 50 mg was used. It was shown that adsorption of the Bismarck Brown (BB) and Disulfine Blue (DSB) follows the pseudo-second-order rate equation, while the Langmuir model explains equilibrium data. Isotherms had also been used to obtain the thermodynamic parameters such as free energy (ΔG^0), enthalpy (ΔH^0) and entropy (ΔS^0) of adsorption. The negative value of (ΔG^0 , ΔH^0 and ΔS^0) confirmed the sorption process was endothermic reflects the affinity of multi walled carbon nanotubes functionalized towards Bismarck Brown (BB) and Disulfine Blue (DSB). A maximum adsorption capacity in binary-component system (6.67 mg/g for Bismarck Brown (BB), and 9.36 mg/g for Disulfine Blue (DSB)).

Keywords: Adsorption capacity; Bismarck Brown; Disulfine blue; Isotherms; thermodynamic.

1. INTRODUCTION

Dyes and pigments have been extensively released in the wastewaters from different industries, particularly from textile, paper, rubber, plastic, leather, cosmetic, food, and

drug industries. These dyes can cause allergic dermatitis, skin irritation, cancer and mutation in living organisms. It also causes eye burns, which may be

*Corresponding author: geramialireza42@gmail.com

responsible for permanent injury to the eyes of human and animals. On inhalation, it can give rise to short periods of rapid or difficult breathing, while ingestion through the mouth produces a burning sensation and may cause nausea, vomiting, profuse sweating, mental confusion, painful micturition, and methemoglobinemia-like syndromes [1,2]. Because of their synthetic natures and complex aromatic molecular structures, dyes are almost non-biodegradable in the ecosystem [3]. The importance of the potential pollution of dyes and their intermediates has been incited with the toxic nature of many dyes, different mutagenic effects, skin diseases and skin irritation and allergies. Moreover, they are dangerous because their microbial degradation compounds, such as benzidine or other aromatic compounds have carcinogenic effect [4].

Azo dyes are divided according to the presence of azo bonds ($-N=N-$) in the molecule; these include mono azo, diazo, triazoetc [5]. Azo dyes resist the effect of oxidation agents and light, thus they cannot be completely treated by conventional methods of anaerobic digestion [6]. It is necessary to find an effective method for the treatment of Bismarck Brown (Table.1). The degradation of Bismarck brown dye in the presence of aqueous zinc oxide suspension has been reported before [7].

It shows several side effects such as eye and skin sensitivity. Also, inhalation of its dust may cause digestion and respiratory tract irritation. Disulfine blue (DSB) (table.1), is a hazardous dye that is widely used for dyeing of wool and silk, carbon paper, cosmetics, and leather [8,9].

Adsorption is one of the best and simple techniques for the removal of toxic and noxious impurities in comparison to other conventional protocols like chemical coagulation, ion exchange, electrolysis, biological treatments is related to

advantages viz. lower waste, higher efficiency and simple and mild operational conditions. Adsorption techniques also have more efficiency in the removal of pollutants which are highly stable in biological degradation process through economically feasible mild pathways [10-12]. The best figures of merit in multi component dyes systems removal are based on development of novel method that permits their accurate simultaneous determination in mixtures. The encounter difficulties are serious peaks overlapping that subsequently impossible their direct determination in mixture using general equation like Beer-Lambert. Derivative spectroscopy efficiently is applicable to resolve absorption peaks overlap through their separation and correction of background interferences. This method is based on searching the wavelengths that possible the accurate and repeatable monitoring of each species in complex matrices without any interference from other target compounds [13, 14]. Hence, it has been extensively used for removal of different chemicals from aqueous solutions [15-17]. Of these methods, nanomaterial's based adsorbents is highly recommended for dyes pollutants removal [18, 19]. The efficient applicability of an adsorption process mainly depends on the physical and chemical characteristics of the adsorbent, which is expected to have high adsorption capacity and to be recoverable and available at economical cost. Currently, various potential adsorbents have been implemented for removal of specific organics from water samples. In this regard, magnetic nanoparticles (MNPs) have been studied extensively as novel adsorbents with large surface area, high adsorption capacity and small diffusion resistance. For instance, they have been used for separation of chemical species such as environmental pollutants, metals, dyes, and gases [20-22].

In this work, MWCNT was modified with Schiff base-like structure following its reaction with N-(3-nitro-benzylidene)-N-trimethoxysilylpropyl-ethane-1, 2-diamine (NBATSPED-MWCNT) as a novel adsorbent followed by the characterization using different techniques such as Fourier transform infrared spectroscopy (FTIR), X-ray diffraction (XRD) and scanning electron microscopy (SEM). This adsorbent was used for the ultrasound-assisted removal of (BB), and (DSB) from aqueous solutions [23]. Therefore, we were motivated to prepare NBATSPED-MWCNT as an alternative to expensive or toxic adsorbents for the removal of (BB), and (DSB) from wastewater. The experimental conditions, such as pH of solution, contact time, initial dyes concentration, and adsorbent dosage as well as the dyes removal percentage as response, were studied and optimized. Various isotherm models, such as Langmuir, Freundlich, Tempkin, and Dubinin–Radushkevich were used to fit the experimental equilibrium data. The results showed the suitability and applicability of the Langmuir model. Kinetic models, such as pseudo-first-order, pseudo-second-order diffusion models indicated that the pseudo-second-order model controls the kinetic of adsorption process. It was shown that the NBATSPED-MWCNT can be effectively used to remove the cationic dyes of (BB), and (DSB) from wastewater.

2. EXPERIMENTAL

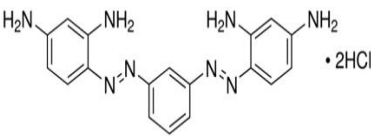
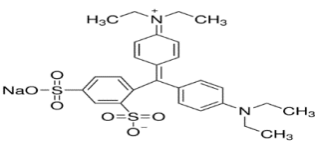
2.1. Reagents and instruments

Disulfine blue, Bismarck Brown activated carbon, sodium hydroxide, hydrochloric acid, activated carbon, sodium hydroxide, hydrochloric acid, N-(3-(trimethoxysilyl)propyl)ethylenediamine (TSPED) and 2-nitrobenzaldehyde (NBA) were purchased from Sigma-Aldrich. Multiwalled carbon nanotubes (MWCNTs). They were supplied from Merck (Darmstadt, Germany). The morphology of samples was studied by scanning electron microscopy (SEM: KYKY-EM 3200, Hitachi Company, China) under an acceleration voltage of 26kV). An ultrasonic bath with heating system (Tecno-GAZ Company SPA Ultrasonic System, Italy) at frequency of 40 kHz and power of 130W was used for the ultrasound-assisted adsorption. The pH/Ion meter (model-728, Metrohm Company, Switzerland, Swiss) was used for the pH measurements. Dyes concentrations were determined using Jasco UV–Vis spectrophotometer model V-530 (Jasco Company, Japan).

2.2. Preparation of NBATSPED-MWCNT

At first step, trimethoxysilylpropylethylene diamine supported on MWCNT (NH₂-MWCNT) was synthesized by the reaction of 1.8 mL N-(3-(trimethoxysilyl)propyl) ethylenediamine, and 0.1 g MWCNT in 20

Table 1. Some characteristics of the investigated dyes

Characteristic	Days	
	Bismarck Brown	Disulfine Blue
Molecular formula	C ₁₈ H ₁₈ N ₈ .2HCl	C ₂₇ H ₃₁ N ₂ NaO ₇ S ₂
Molecular weight	419.31 (g mol ⁻¹)	210.2 (g mol ⁻¹)
Chemical structure		

mL of dichloromethane under reflux at 40°C in the oil bath for 24 hours. Then, the obtained solid was filtered, rinsed sequentially with ethanol and dried in an oven at 50°C. Then, 0.9 g of 2-nitrobenzaldehyde was added to the resulting substance in 20 mL of methanol and refluxed at 60°C in oil bath for 24 hours. The product was filtered, washed with 50 mL of ethanol, distilled water and then dried in oven for 10 h 50°C. In this way, N-(3-nitro-benzylidene)-N0-trimethoxysilylpropyl-ethane-1, 2-diamine supported on MWCNT (NBATSPED-MWCNT) was obtained as a new adsorbent. The steps for the synthesis of the adsorbent are presented in Scheme 1[24].

2.3. Adsorption of (BB), and (DSB) on to NBATSPED-MWCNT.

A batch process using NBATSPED-MWCNT in presence of ultrasound was applied for binary adsorption of (BB), and (DSB), while all experiments were under taken in a cylindrical glass vessel by adding 0.05 g of adsorbent to 10 ml of PH 8.0 for (BB), and PH 6.0 for (DSB) as optimum value. The vessel was immersed in an ultrasonic bath for 4 min at room temperature and subsequently the solutions were centrifuged. Then non-adsorbed dye contents were determined by using UV-Vis spectrophotometer set at wavelengths 448 nm for (BB), and 650 for (DSB), respectively.

2.4. Batch adsorption dyes adsorption process

Batch adsorption experiments were carried out to determine the (BB), and (DSB) adsorption isotherm onto N-(3-nitro-benzylidene)-N-trimethoxysilylpropyl-ethane-1,2-diamine (NBATSPED-MWCNT) composite and its thermodynamic properties: 500 mL solution having 100 mg/L concentration of

(BB), and (DSB) was prepared and Initial pH of the solution was adjusted with the help of 0.01N HCl / 0.01N NaOH aqueous solution without any further adjustments during the experiments. 10 samples of 50 mL solution were taken in ten 250 mL flasks containing fixed adsorbent dose of 25 mg/L. These flasks were agitated at a constant rate of 200 rpm in a temperature controlled orbital shaker maintained at 25°C temperatures. One of the sample flasks was withdrawn from orbital shaker after fixed time intervals (10, 20, 30, 40, 50, 60, and 70 at 120 min) and analyzed for remaining metal ions present in the adsorbate solution. N-(3-nitro-benzylidene)-N-tri methoxy silylpropyl-ethane-1, 2-diamine (NBATSPED-MWCNT) was separated from aqueous solution by filtration through whatman No. 42 filter paper. The Bismarck (BB), and (DSB) concentration in the solution was measured using a double beam UV-Vis spectrophotometer (Jasco, Model UV-Vis V-530, Japan) set at wavelengths 448 nm for (BB), and 650 for (DSB). The amount of adsorbed dyes at equilibrium (q_e (mg/g)) was calculated using equation:

$$R\% = \frac{C_0 - C_e}{C_0} \times 100 \quad (1)$$

Where C_0 (mgL⁻¹) and C_t (mgL⁻¹) is the concentration of target at initial and after time t respectively.

$$q_i = \frac{V(C_0 - C_e)}{M} \times 100 \quad (2)$$

where C_0 (mgL⁻¹) and C_e (mgL⁻¹) are the initial dye concentration and equilibrium dyes concentration in aqueous solution, respectively, V (L) is the solution volume and W (g) is the adsorbent mass.

3. RESULTS AND DISCUSSION

3.1. Characterization of adsorbent

The FTIR spectrum of NBATSPED-MWCNTs (Fig. 2), shows absorption peak

at 1715 cm^{-1} corresponding to the Stretching vibration of carbonyl groups. The broad peaks at 1086 cm^{-1} could be assigned to C–O stretching from phenolic, alcoholic, etheric groups and to C–C bonds. The new peak appearing at 3400 cm^{-1} corresponds to OH stretching. This peak can be assigned to the hydroxyl group of moisture, or carboxylic groups. The aromatic C=C stretch is observed at 1459 cm^{-1} . The FT-IR spectrum of NH_2 -MWCNT (Fig. 2) displays a new peak as a weak shoulder at 2931 cm^{-1} , which corresponds to the stretching vibrations of C–H bonds in propyl group. After the addition of 2-nitrobenzaldehyde, the new peak appeared at 1635 cm^{-1} is related to C=N which indicates successful synthesis of NBATSPED. Following the addition of NBA (Fig. 3), two peaks at 1324 and 1585 cm^{-1} are attributed to $-\text{NO}_2$ groups which confirm again the success of this step [25]. The morphological features of the samples studied by SEM are shown in Fig.3a) and b. MWCNTs are observed to be smooth, homogeneous, tidy and approximately uniform in size distribution (Fig.3a). After the surface modification with NBATSPED, the NBATSPED-functionalized MWCNTs became rough, larger and bundled (Fig. 3b) [26]. The XRD pattern of the NBATSPED-

MWCNTs (Fig. 3b) represents a peak at 25.961 (002) corresponding to the interlayer spacing of the nanotube. The peaks at $43.05(100)$, $53.92(004)$, and $78.5(100)$ correspond to diffractions and reflections from the carbon atoms [26] As seen, the highly crystalline nature of the MWCNTs after functionalizing with NBATSPED is confirmed, while the high intensity of peak at 53.49 (004) shows that there has been a small amount of material in amorphous state. The observed XRD pattern indicates that the prepared NBATSPEDMWCNT is well-synthesized.

3.2. Effect of pH

The pH has been identified as one of the most important parameter that is effective on dyes sorption. The effect of pH on the (BB), and (DSB) onto NBATSPED-MWCNTs was studied at pH 2.0–10.0, Fig.4. The maximum sorption was observed at pH 8.0 for (BB), and pH 6.0 for (DSB). Therefore, the remaining all sorption experiments were carried out at this pH value. The sorption mechanisms on the NBATSPED-MWCNTs surface reflect the nature of the physic chemical interaction of the solution [27, 28]. At highly acidic pH, the overall surface charge on the active sites became. Positive

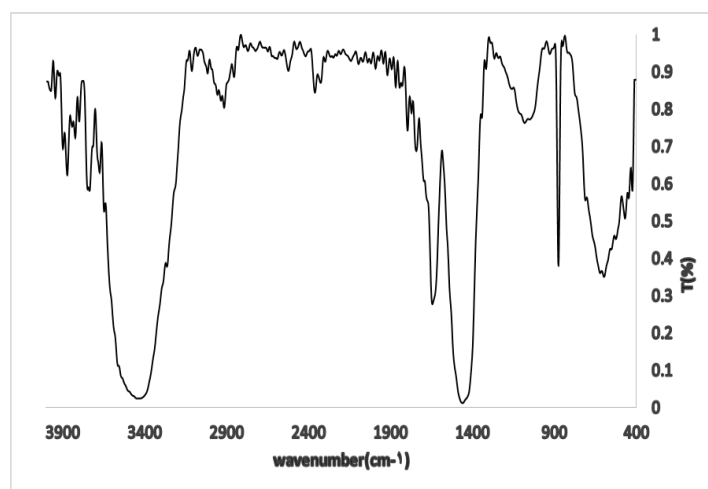


Fig. 2. FT-IR transmittance spectrum of the prepared NBATSPED-MWCNT.

and (BB), and (DSB) and protons compete for binding sites on NBATSPED-MWCNTs, which results in lower uptake of (BB), and (DSB). The sorbent surface was more negatively charged as the pH solution increased from pH 8.0 for (BB) and pH 6.0 for (DSB). The functional groups of the NBATSPED-MWCNTs was more deprotonated and thus available for the (BB), and (DSB). Decrease in sorption

yield at higher pH=8 and pH=6 for the (BB), and (DSB) is not only related to the formation of soluble hydroxylase complexes of the (BB), but also to the ionized nature of the NBATSPED-MWCNTs of the sorbent under the studied pH. Previous studies also reported that the maximum sorption efficiency of (BB), and (DSB) on biomass was observed at pH (8.0 and 6.0).

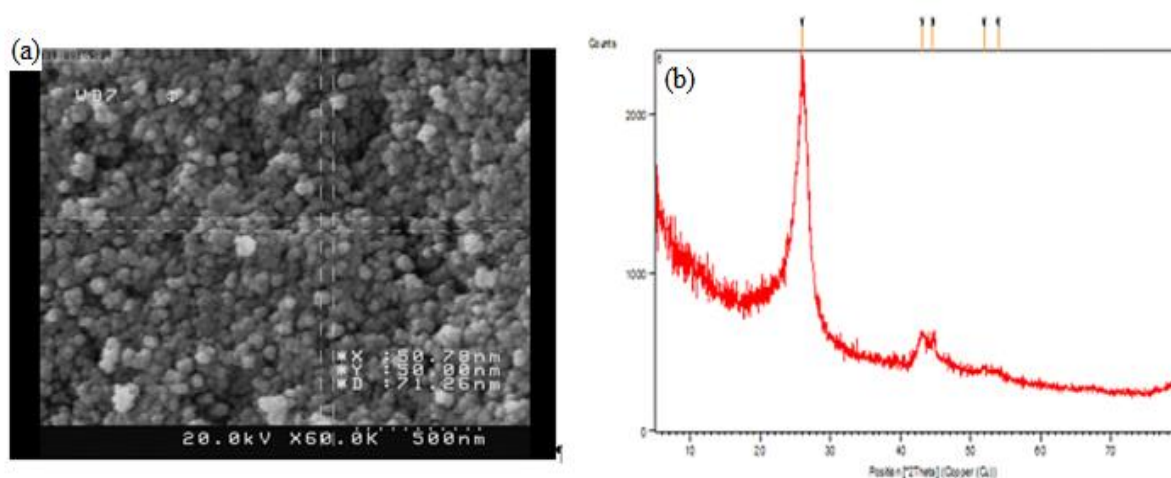


Fig. 3. The (a) SEM image and (b) XRD of the prepared NBATSPED-MWCNT.

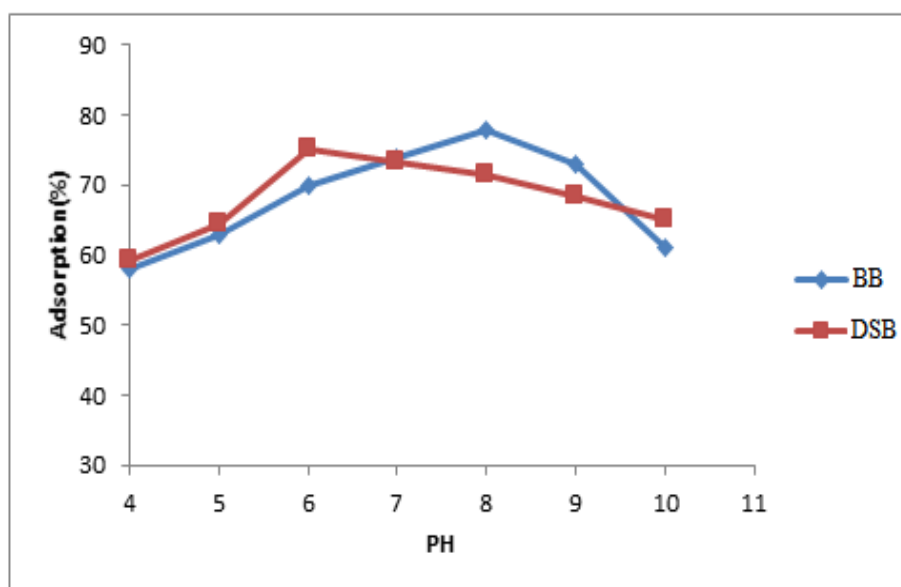


Fig. 4. Effect of initial solution pH on the adsorption amount of (BB), and (DSB) onto NBATSPED-MWCNTs.

3.3. Effect of sorbent dosage

The sorbent dosage is an important parameter because this determines the capacity of a sorbent for a given initial concentration. The sorption efficiency for (BB), and (DSB) as a function of sorbent dosage was investigated. The percentage of the metal sorption steeply increases with the sorbent loading up to 50 mg Fig.5. This result can be explained by the fact that the sorption sites remain unsaturated during the sorption reaction, whereas the number of sites available for sorption site increases by increasing the sorbent dose [29]. The maximum sorption was attained at sorbent dosage, 50 mg. Therefore, the optimum sorbent dosage was taken as 50 mg for further experiments. This can be explained by when the sorbent ratio is small, the active sites for binding metal ions on the surface of NBATSPED-MWCNTs is less, so the sorption efficiency is low. As the sorbent dose increased, more active sites to (BB), and (DSB), thus it results an increase in the sorption efficiency until saturation.

3.4. Effect of contact time

The effect of contact time on the adsorption capacity of (BB), and (DSB) onto NBATSPED-MWCNTs is shown in (Fig. 6). When the initial (BB), and (DSB) concentration is increased from 1 to 15 mg/L the amount of (BB), and (DSB) adsorbed onto NBATSPED-MWCNTs, 10 at 120 min contact time, pH value 8 for Bismarck Brown(BB) and pH value 6 for (DSB), 5mg adsorbent dose and the constant temperature 298.15 K. The increase of loading capacity of NBATSPED-MWCNTs with increasing initial dyes concentration may be due to higher interaction between (BB), and (DSB) dyes and adsorbent [30,31]. These results show that rapid increase in

adsorbed amount of (BB), and (DSB) is achieved during the first 65 minutes. Similar results were reported before for the removal of hazardous contaminants from wastewater.

3.5. Effect of temperature

To study the effects of temperature on the adsorption of dyes by NBATSPED-MWCNTs, the experiments were performed at temperatures from 298.15 to 328.15 K. Fig.7, shows the influence of temperature on the adsorption of dye on NBATSPED-MWCNTs. As it was observed, the equilibrium adsorption capacity of (BB), and (DSB) onto NBATSPED-MWCNTs was found to increase with increasing temperature. This fact indicates that the mobility of dyes molecules increased with the temperature, additionally the viscosity of dyes solution reduces with rise in temperature and as a result, it increases the rate of diffusion of dyes molecules. The results were in agreement with the effect of the solution pH, and temperature on adsorption behavior of reactive dyes on activated carbon [32, 33].

3.6. Adsorption equilibrium study

Adsorption equilibrium isotherm is designed based on mathematical relation of the amount of adsorbed target per gram of adsorbent (q_e (mg/g)) to the equilibrium non-adsorbed amount of dyes in solution (C_e (mg/L) at fixed temperature [34, 35]. Isotherm studies are divided to well-known models such as Langmuir, Freundlich, Temkin and Dubinin–Radushkevich based on well-known conditions. The Langmuir model is the most frequently employed model given by following equation [36]:

$$q_e = \frac{Q_m K_1 C_e}{1 + K_1 C_e} \quad (3)$$

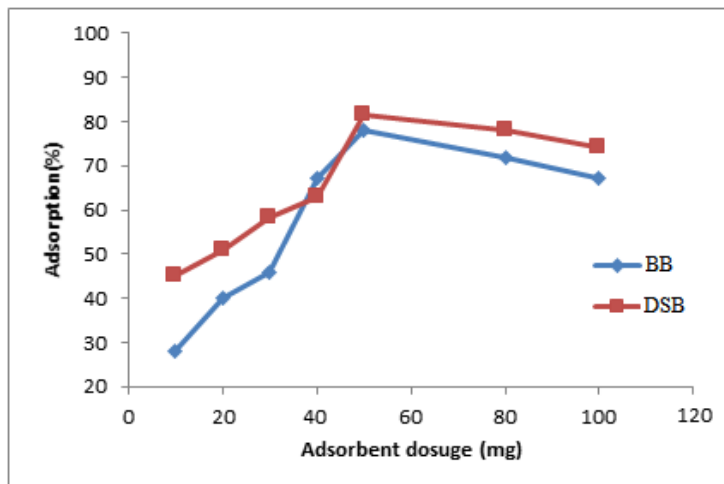


Fig. 5. Effect of dosage NBATSPED-MWCNTs on the adsorption amount of (BB), and (DSB).

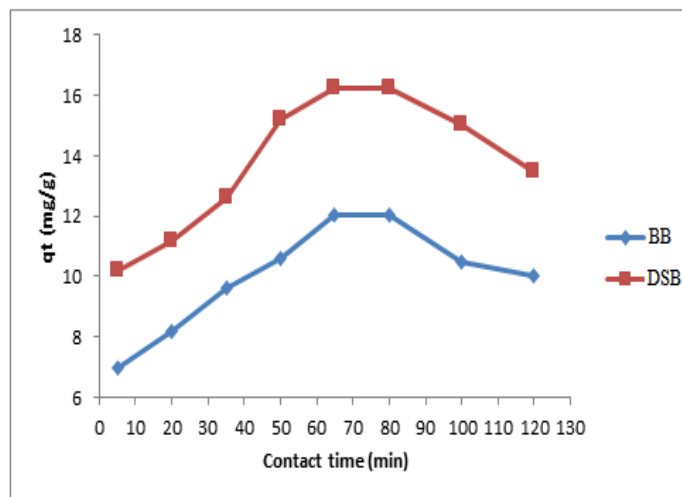


Fig.6. Effect of contact time on the adsorption of Bismarck Brown (BB) and Disulfine Blue (DSB) dyes by NBATSPED-MWCNTs.

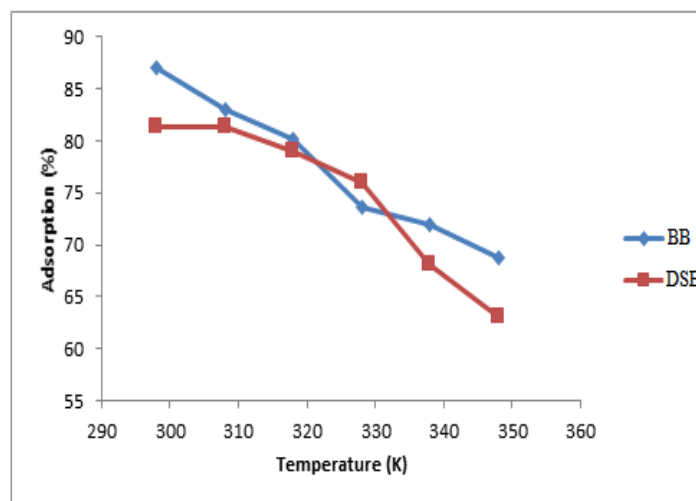


Fig.7. Effect of temperature on the adsorption amount of (BB), and (DSB) on NBATSPED-MWCNTs.

Where C_e , Q_m and K_L are the concentration of adsorbate at equilibrium (mg/L), maximum monolayer adsorption capacity (mg/g) and Langmuir constant (L/mg), respectively. C_e/q_e was plotted against C_e where parameters such as Q_m , K_L , and R^2 were calculated based on the slope and intercept of such lines and displayed in (Table. 1). The values of K_a (the Langmuir adsorption constant (L/mg)) and Q_m (theoretical maximum adsorption capacity (mg/g)) were obtained from the intercept and slope of the plot of C_e/q_e versus C_e , respectively. The applicability of Langmuir model for the interpretation of the experimental data over the whole concentration range is proven from high correlation coefficient at all adsorbent masses. The increase in the amount of adsorbent leads to significant enhancement in the actual amount of adsorbed dyes. The parameters of Freundlich isotherm model such as K_F and the capacity of the adsorption were calculated from the intercept and slope of the linear plot of $\ln q_e$ versus $\ln C_e$, respectively. The heat of the adsorption

and the adsorbent–adsorbate interaction were evaluated by using Temkin isotherm model. In this model, B is the Temkin constant related to heat of the adsorption (J/mol), T is the absolute temperature(K), R is the universal gas constant (8.314J/mol. K) and K is the equilibrium binding constant(L/mg). D–R model was applied to estimate the porosity apparent free energy and the characteristic of adsorption [37, 38]. In this model B (mol^2/kJ^2) is a constant related to the adsorption energy, Q_s (mg/g) is the theoretical saturation capacity and E is the Polanyi potential. The slope of the plot of $\ln q_e$ versus ε^2 gives B and its intercept yields the Q_s value. The linear fit between the plot of C_e/q_e versus C_e and calculated correlation coefficient (R^2) for Langmuir isotherm model shows that the dyes removal isotherm can be better represented by Langmuir model (Table. 1). This confirms that the adsorption of dyes takes place at specific homogeneous sites as a monolayer on to the NBATSPED-MWCNTs surface.

Table. 1. Various isotherm constants and correlation coefficients calculated for the adsorption of dyes onto NBATSPED-MWCNTs.

Isotherm	Equation	parameters	Value of parameters For BB	Value of parameters For DSB
Langmuir	$q_e = q_m b C_e / (1 + b C_e)$	Q_m (mg g ⁻¹)	6.67	9.36
		K_a (L mg ⁻¹)	0.31	0.208
		R^2	0.950	0.9740
Freundlich	$\ln q_e = \ln K_F + (1/n) \ln C_e$	n	0.536	0.617
		K_F (mg) ¹⁻ⁿ L ⁿ g ⁻¹	2.9	2.0
		R^2	0.8722	0.8719
Tempkin	$q_e = B_T \ln K_T + B_T \ln C_e$	B_T	12.6	10.5
		K_T (L mg ⁻¹)	1.3	1.1
		R^2	0.4916	0.6071
Dubinin-Radushkevich (DR)	$\ln q_e = \ln Q_d - B \varepsilon^2$	Q_d (mg g ⁻¹)	20.8	15.2
		$K_D \times 10^{-7}$ (mol/J) ²	6.0	6.0
		E (kJ mol ⁻¹)	-903.7	-903.7
		R^2	0.742	0.781

3.7. Kinetic study

Adsorption of a solute by a solid in aqueous solution through complex stages [39] is strongly influenced by several parameters related to the state of the solid (generally with very heterogeneous reactive surface) and to physico-chemical conditions under which the adsorption occurred. The rate of dyes adsorption onto adsorbent was fitted to traditional models like, pseudo-first, pseudo-second-order and Elovich models. The Lagergren pseudo-first order modeled described the adsorption kinetic data [40]. The Lagergren is commonly expressed as follows:

$$\frac{dq_t}{dt} = k_1(q_e - q_t) \quad (4)$$

Where q_e and q_t (mg/g) are the adsorption capacities at equilibrium and at time t , respectively. k_1 is the rate constant of the pseudo-first-order adsorption (L/min). The $\log(q_e - q_t)$ versus t was plotted and the values of k_1 and q_e were determined by using the slope and intercept of the line, respectively.

$$\log(q_e - q_t) = \log q_t - \left(\frac{k_1}{2.303}\right)t \quad (5)$$

The fact that the intercept is not equal to q_e imply that their action is unlikely to follow the first-order. The relationship between initial solute concentration and rate of adsorption is linear when pore diffusion limits the adsorption process. Therefore, it is necessary to fit experimental data to another model (Table 4) such as pseudo-second order model [41], based on the following equation:

$$\frac{dq_t}{dt} = k_2(q_e - q_t)^2 \quad (6)$$

Eq. (18) is integrated over the interval 0 to t for t and 0 to q_t for q_t , to give

$$\frac{t}{q_t} = \frac{1}{k_2 q_e^2} + \frac{t}{q_e} \quad (7)$$

As mentioned above, the plot of $\log(q_e - q_t)$ versus t does not show good results for entire sorption period, while the plot of t/q_t versus t shows a straight line. The values of k_2 and equilibrium adsorption capacity (q_e) were calculated from the intercept and slope of the plot of t/q versus t (Table. 2). The calculated q_e values at different working conditions like various initial dyes concentrations and/or adsorbent masses were close to the experimental data and higher R^2 values corresponding to this model confirm its more suitability for the explanation of experimental data. This indicates that the pseudo-second-order kinetic model applies better for the adsorption of (BB), and (DSB) system for the entire sorption period the Intraparticle diffusion equation is given as [42]:

$$q_t = k_{dif} t^{1/2} + C \quad (8)$$

Where k_{dif} is the intraparticle diffusion rate constant (mg/(g. min^{1/2})) and C shows the boundary layer thickness. The linear form of Elovich model is generally expressed as [43]:

$$q_t = \frac{1}{\beta} \ln(\alpha\beta) + \frac{1}{\beta} \ln t \quad (9)$$

The kinetic data from pseudo-first and pseudo-second-order adsorption kinetic models as well as the intraparticle diffusion and Elovich model are given in Table 4. The linear plots of t/q_t versus t indicated a good agreement between the experimental and calculated q_e values for different initial dyes concentrations. Furthermore, the correlation coefficients of the pseudo-second-order kinetic model ($R^2 = 0.9831$, $R^2 = 0.9891$) were greater than that of the pseudo-first-order model ($R^2 = 0.8676$, $R^2 = 0.99783$) for (BB), and (DSB) respectively. As a result, the adsorption fits to the pseudo-second-order better than the pseudo-first-order kinetic model.

Table 2. Kinetic parameters for the adsorption of dyes onto NBATSPED-MWCNTs

Model	Parameters	Value of parameters for BB	Value of parameters for DSB
pseudo-First-order kinetic	k_1 (min-1)	0.03	0.065
	q_e (calc) (mg g ⁻¹)	6.2	16.0
	R^2	0.9783	0.8676
pseudo-Second-order kinetic	k_2 (min-1)	8.0	5.2
	q_e (calc) (mg g ⁻¹)	13.25	18.62
	R^2	0.9831	0.9891
Elovich	β (g mg-1)	0.53	0.3
	α (mg g-1 min-1)	11.2	6.43
	R^2	0.899	0.9497
	q_e (exp) (mg g ⁻¹)	12.04	16.4

3.9. Adsorption thermodynamics

The thermodynamic parameters, namely Gibbs free energy change (ΔG°), enthalpy change (ΔH°) and entropy change ΔS° , for the adsorption processes were determined using the following equations [44]:

$$\Delta G^\circ = -RT \ln K_{ad} \quad (10)$$

$$\ln K_{ad} = \frac{-\Delta H^\circ}{RT} + \frac{\Delta S^\circ}{R} \quad (11)$$

A graph (Fig. 8) is developed from a plot of $\ln K_e$ against $1/T$, from the slope of which ΔG can be procured. In Table. 3 and 4, the summary of the thermodynamic parameter outcomes for the adsorption of (BB), and (DSB) onto derived NBATSPED-MWCNTs at different temperatures is shown.

Via applying the equation adsorption of (BB), and (DSB), the ΔG° values were computed. As shown in Fig. 8, upon the increase in the temperature from 298 to 348 K, NBATSPED-MWCNTs adsorbent diminished, and exothermicity nature of the process was confirmed. The values of the thermodynamic parameters (Table 5 and 6) [45] were computed using the plots. The feasibility and spontaneity nature of the process was revealed by the negative value of ΔG° . On the other hand, the exothermicity nature of adsorption was proven by the negative value of ΔH° and

the value of ΔS° was a good indication of change in the randomness at the derived NBATSPED-MWCNTs solution interface during the sorption. The fact that ΔG° values up to -4.7 kJ/mol (BB), and -3.65 kJ/mol (DSB) are accordant with electrostatic interaction between sorption sites and the (BB), and (DSB) (physical adsorption) has been reported. The obtained ΔG° values in this article for (BB), and (DSB) are <-5 kJ/mol suggesting the predominancy of the physical adsorption mechanism in the sorption process [44,45].

4. CONCLUSION

The N-(3-nitro-benzylidene)-N-trimethoxysilylpropyl-ethane-1,2-diamine onto multi walled carbon nanotubes(NBATSPED-MWCNTs) has been synthesized and used as an effective adsorbent for the removal of (BB), and (DSB) dyes from aqueous solutions. The effects of adsorbent dosage, pH, contact time, and initial dyes on the removal of (BB), and (DSB) were investigated through batch experiments. Isotherm models such as Langmuir, Freundlich, Temkin, and Dubinin-Radushkevich for the adsorption process were evaluated and the equilibrium data were best described by the Langmuir model. The process kinetics was found to be successfully fitted

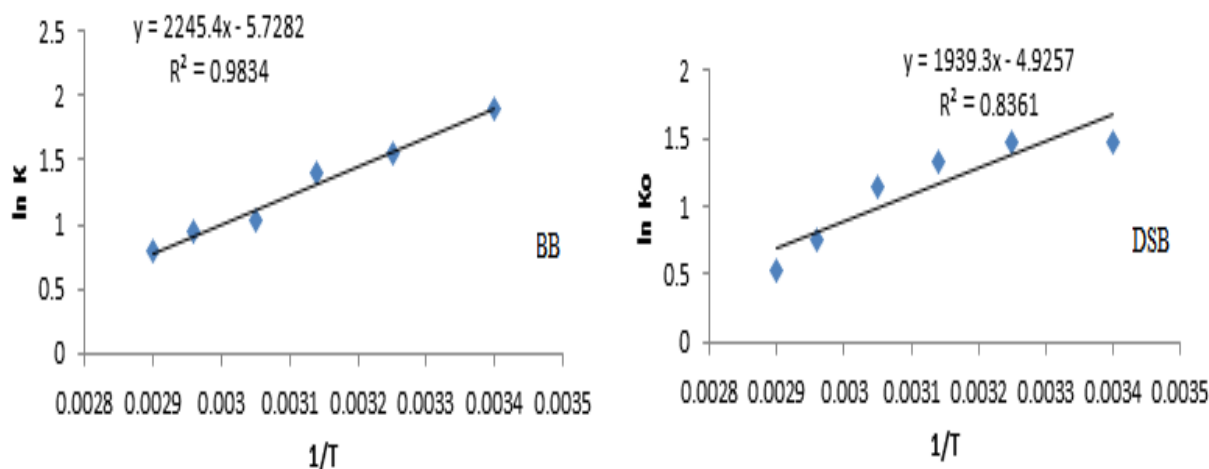


Fig. 8. Plot of $\ln K_c$ vs. $1/T$ for the estimation of thermodynamic parameters.

Table 3: The distribution coefficients at different temperature

Dyes (mg/L)	R^2	K_d					
		298K	308K	318K	328K	338K	348K
(BB) 10(mg/L)	0.983	6.7	4.5	4.0	2.8	2.6	2.2
(DSB) 10(mg/L)	0.836	4.4	4.4	3.8	3.2	2.1	1.7

Table 4. The thermodynamic parameters for the adsorption of (BB), and (DSB) onto NBATSPED-MWCNTs adsorbent

Dyes (mg/L)	ΔH° (kJ/mol)	ΔS° (kJ/mol K)	ΔG° (kJ/mol)					
			298K	308K	318K	328K	338K	348K
(BB) 10(mg/L)	-18.66	-47.7	-4.7	-4.0	-3.7	-2.8	-2.64	-2.3
(DSB) 10(mg/L)	-16.17	-40.1	-3.65	-3.78	-3.5	-3.18	-2.18	-1.56

to the pseudo-second-order kinetic model. Adsorption of (BB), and (DSB) was found to be spontaneous at the temperatures under investigation. The negative value of (ΔG° , ΔH° and ΔS°) confirmed the sorption process was endothermic. The goal for this work is to develop inexpensive, highly available, effective (BB), and (DSB) dyes adsorbents from natural waste as alternative to existing commercial adsorbents. NBATSPED-MWCNTs has a high adsorption capacity when compared to other adsorbents for (BB), and (DSB) dyes removal from an aqueous medium.

ACKNOWLEDGEMENT

The authors gratefully acknowledge partial support of this work by the Islamic Azad University, Branch of Dashtestan, Iran.

References

- [1] B.H. Hameed, D.K. Mahamoud, A.L. Ahmad, J. Hazard. Mater.158, 65 (2008).
- [2] S.A. Haji Azaman, A. Afandi, B.H. Hameed, A.T. Mohd Din, J. Appl. Sci. Eng. 21(3), 317 (2018).
- [3] A. Reghioua, D. Barkat, A.H. Jawad, A.S. Abdulhameed, A.A. Al-Kahtani, A.A. Al-Othman, J. Environ. Chem. Eng. 9, 105166 (2021).

- [4] G. Absalan, A. Bananejad, M. Ghasemi, *Anal. Bioanal. Chem. Res.* 4, 65 (2017).
- [5] S. Bagheri, *Orient. J. Chem.* 32, 549 (2016).
- [6] Gh. Vatan khah, A. Kohmareh, J. *Phys. Theore. Chem.* 14, 237 (2018).
- [7] F. H. Hussein, M.H. Obies, A.A. Ali Drea, *Int. J. Chem. Sci.* 8, 2763 (2010).
- [8] F. Marahel, B. Mombeni Goodajdar, N. Basri, L. Niknam, A.A. Ghazali, *Iran. J. Chem. Chem. Eng.* 41, 2358 (2022).
- [9] A. R. Parvizi, B. Bagheri, N. Karachi, L. Niknam, *Orient. J. Chem.* 32, 565 (2017).
- [10] A. Asfaram, M. Ghaedi, F. Yousefi, M. Dastkhoon, *Ultrason Sonochem.* 33, 77 (2016).
- [11] Sh. Davoudi, *Iran. J. Chem. Chem. Eng.* 41(7): 2343 (2022).
- [12] Sh. Einolghozati, E. Pournamdari, N. Choobkar, F. Marahel, *J. Appl. Chem. Res.* 17, 47 (2023).
- [13] M. Pargari, F. Marahel, B. Mombini Godajdar, *Desal. Water Treat.* 212, 164 (2021).
- [14] [14] F. Marahel, B. Mombeni Goodajdar, L. Niknam, M. Faridnia, E. Pournamdari, S. Mohammad Doost, *Int. J. Environ. Anal. Chem.* 101, 11 (2021).
- [15] Sh. Einolghozati, E. Pournamdari, N. Choobkar, F. Marahel, *Desal. Water Treat.* 278, 195 (2022).
- [16] M. Kiani, S. Bagheri, A. Khalaji, N. Karachi, *Desal. Water Treat.* 226, 147 (2021).
- [17] A. Geramizadegan, *J. Phys. Theore. Chem.* 18, 1 (2022).
- [18] J. Luan, P.-X. Hou, C. Liu, C. Shi, G. X. Li, H.-M. Cheng, *J. Mater. Chem. A.* 4, 1191 (2016).
- [19] Y. Liu, G. Cui, C. Luo, L. Zhang, Y. Guo, S. Yan, *RSC Adv.* 4, 55162 (2014).
- [20] S.H. Ahmadi, P. Davar, A. Manbohi, *Iran. J. Chem. Chem. Eng.* 35, 63 (2016).
- [21] R. Manohar, V.S. Shrivastava, *J. Mater. Environ. Sci.* 6, 11 (2015).
- [22] L. Niknam, Sh. Davoudi, *J. Phys. Theore. Chem.* 18, 37 (2022).
- [23] F. Raoufi, H. Aghae, M. Monajjemi, *Orient. J. Chem.* 32, 1839 (2016).
- [24] H. Aghae, F. Raoufi, *Orient. J. Chem.* 33, 2542 (2017).
- [25] N. Karachi, S. Motahari, S. Nazarian, *Desal. Water Treat.* 228, 389 (2021).
- [26] M. Kiani, S. Bagheri, N. Karachi, E. Alipanahpour Dil, *Desal. Water Treat.* 152, 366 (2019).
- [27] H. Z. Khafri, M. Ghaedi, A. Asfaram, M. Safarpour, *Ultrason. Sonochem.* 38, 371 (2017).
- [28] M. Turabik, *J. Hazard. Mater.* 158, 52 (2008).
- [29] S. Hajati, M. Ghaedi, H. Mazaheri, *Desal. Water Treat.* 57, 3179 (2016).
- [30] Sh. Bouroumand, F. Marahel, F. Khazali, *Desal. Water Treat.* 223, 388 (2021).
- [31] F. Marahel, *Iran. J. Chem. Chem. Eng.* 38, 129 (2019).
- [32] M. Ali Khan, M. R. Siddiqui, M. Otero, Sh. Ahmed Alshareef, M. Rafatullah, *Polymers.* 12, 500 (2020).
- [33] Y. Zhao, Zh. Li, *J. Mol. Liq.* 293, 111516 (2019).
- [34] N.N. Abd Malek, A.H. Jawad, A.S. Abdulhameed, K. Ismail, B.H. Hameed, *Int. J. Biolog. Macromol.* 146, 530 (2020).
- [35] A. H. Jawad, I.A. Mohammed, A.S. Abdulhameed, *J. Polymers Environ.* 28, 2720 (2020).
- [36] A. Azari, R. Nabizadeh, S. Nasser, A.H. Mahvi, A.R. Mesdaghinia, *Chemospher.* 250, 126238 (2020).
- [37] V. Kumar, P. Saharan, A.K. Sharma, A. Umar, I. Kaushal, Y. Al-Hadeethi, B. Rashad, A. Mittal, *J. Ceram. Int.* 46, 10309 (2020).

- [38] F. Maghami, M. Abrishamkar, B. Mombeni Goodajdar, M. Hossieni, Desal. Water Treat. 223, 388 (2021).
- [39] S. Javad, H. Aghaee, M. Ghaedi, Orient. J. Chem. 30, 1883 (2014).
- [40] H. Esmaeilli, F. Foroutan, D. Jafari, Korean. J. Chem. Eng. 37, 804 (2020).
- [41] X. Tao, Sh. Wang, Zh. Li, J. Environ. Manage. 255, 109834 (2020).
- [42] S. Hajati, M. Ghaedi, B. Barazesh, F. Karimi, R. Sahraei, A. Daneshfar, A. Asghari, J. Ind. Eng. Chem. 20, 2421 (2014).
- [43] M. Hubbe, S. Azizian, S. Douven, A Review. Bio Resource. 14, 7582 (2019).
- [44] H. S. Ghazimokri, H. Aghaie, M. Monajjemi, M.R. Gholami, Russian J. Phys. Chem. A. 96, 371 (2022).
- [45] E. Mousavi, A. Geramizadegan, J. Phys. Theor. Chem. 17, 123 (2021).

حذف بیسمارک قهوه‌ای و دی سولفین آبی از محلول‌های آبی با استفاده از بر روی MWCNT های
عامل دار شده توسط $N-(3\text{-nitrobenzylidene})\text{-}N'\text{-trimethoxysilylpropyl-ethane-1,2-diamine}$

علیرضا گرامی زادگان*

دانشگاه آزاد اسلامی، واحد دشتستان، گروه مهندسی شیمی، دشتستان، ایران

چکیده

کاربرد $N-(3\text{-nitro-benzylidene})\text{-}N\text{-trimethoxysilylpropyl-ethane-1,2-diamine}$ بر روی نانولوله های کربنی چند جداره (NBATSPED-MWCNTs) برای حذف بیسمارک براون و دی سولفین آبی از محلول های آبی گزارش شده است. این ماده جدید با تکنیک های مختلفی مانند XRD، SEM و FT-IR مشخص شد. تأثیر دوز نانوذرات، pH محلول نمونه، غلظت رنگ های فردی، زمان تماس بین نمونه و جاذب، دما و قدرت یونی محلول نمونه با انجام یک تکنیک جذب ناپیوسته مورد بررسی قرار گرفت. حداکثر حذف ۱۵ میلی گرم در لیتر از رنگ های منفرد از محلول نمونه آبی در pH 8.0 برای بیسمارک براون و در pH 6.0 برای دی سولفین آبی در 65.0 دقیقه زمانی که مقدار جاذب 50.0 میلی گرم بود به دست آمد. مورد استفاده قرار گرفت. نشان داده شد که جذب بیسمارک براون و دی سولفین آبی از معادله نرخ شبه مرتبه دوم پیروی می کند، در حالی که مدل لانگمویر داده های تعادل را توضیح می دهد. ایزوترم ها همچنین برای به دست آوردن پارامترهای ترمودینامیکی مانند انرژی آزاد (ΔG^0)، آنتالپی (ΔH^0) و آنتروپی (ΔS^0) جذب استفاده شده بودند. مقدار منفی (ΔG^0 ، ΔH^0 و ΔS^0) تایید کرد که فرآیند جذب گرماگیر بود، نشان دهنده میل ترکیبی نانولوله های کربنی چند جداره ای که نسبت به بیسمارک قهوه ای و دی سولفین آبی عمل کرده شده اند. حداکثر ظرفیت جذب در سیستم اجزای دوتایی (۶,۶۷ میلی گرم در گرم برای بیسمارک براون و ۹,۳۶ میلی گرم در گرم برای دی سولفین آبی) بدست آمد.

کلید واژه ها: ظرفیت جذب؛ قهوه ای بیسمارک؛ آبی دی سولفین؛ ایزوترم ترمودینامیکی

* مسئول مکاتبات: geramialireza42@gmail.com